ELSEVIER

Materials Science and Engineering A287 (2000) 183–188

MATERIALS SCIENCE & ENGINEERING A

www.elsevier.com/locate/msea

Sintering, consolidation, reaction and crystal growth by the spark plasma system (SPS)

Mamoru Omori

Institute for Materials Research, Tohoku University, Sendai 980-8577, Japan

Abstract

The graphite die set in spark plasma system (SPS) is heated by a pulse direct current. Weak plasma, discharge impact, electric field and electric current, which are based on this current, induce good effects on materials in the die. The surface films of aluminum and pure WC powders are ruptured by the spark plasma. Pure AlN powder is sintered without sintering additives in the electric field. The spark plasma leaves discharge patterns on insulators. Organic fibers are etched by the spark plasma. Thermosetting polyimide is consolidated by the spark plasma. Insoluble polymonomethylsilane is rearranged into the soluble one by the spark plasma. A single crystal of $CoSb_3$ is grown from the compound powders in the electric field by slow heating. Coupled crystals of eutectic powder are connected with each other in the electric field.

Keywords: Spark plasma system; Spark plasma sintering; Plasma activated sintering; Discharge; Electric field; Discharge impact; Skin current; Sintering; Consolidation; Chemical reaction; Crystal growth

1. Introduction

The spark plasma system (SPS) has been called spark plasma sintering (SPS) [1] or plasma activated sintering (PAS) [2]. Spark plasma system is an appropriate description, because the system enables the sintering of metals and ceramics, the consolidation of polymers, the joining of metals, crystal growth, and chemical reactions. It is suggested that the term spark plasma system includes spark plasma sintering (SPS), spark plasma consolidation (SPC), spark plasma joining (SPJ), spark plasma growth (SPG) and spark plasma reaction (SPR).

SPS was developed based on the idea of using the plasma on electric discharge machine for sintering metal and ceramics in the early 1960s by Inoue et al. They expected that sintering assisted by plasma could help realize advanced materials. The SPS equipment was patented in America [3,4]. Few machines were only sold in America and Japan. In the late 1980s the patent expired, and various companies started to manufacture SPS equipment based on the original techniques.

SPS has been mainly characterized by spark plasma created by a pulse direct current during heat treatment of powders in a graphite die [1,2,5]. There are gaps between the two electrodes in the electric discharge machine, and high-energy plasma is generated there. The die alignment of SPS, however, does not allow any gaps, and high-energy plasma cannot be expected without such gaps. It is reasonable that the plasma of SPS has not been identified directly. Electric noise has been observed, and is thought to correspond to the plasma generation [6].

There are five expected merits of SPS [1,2]: 1, generation of spark plasma; 2, effect of electric field; 3, effect of electric current in the conductor or skin current on the semiconductor and insulator; 4, Impact of spark plasma; 5, rapid heating and cooling. The first is considered as a means for the fabrication of new materials. The second and third effects had not been considered to be significant for sintering and reactions. The fourth effect is due to mechanical pressure caused by spark plasma, and does not seem to be serious. The fifth is the efficiency of heat-treatment. There are no insulators and heating elements of large heat capacity, and the graphite die is heated directly by an electric current. These conditions result in rapid heating and cooling.

Innovative materials have been obtained with ceramics, metals, polymers and semiconductors. Some of them cannot be prepared without SPS. Aluminum metal is solidified like other metals. Pure tungsten carbide and aluminum nitride powders can be sintered

0921-5093/00/$ - see front matter
PII: S0921-5093(00)00773-5

without additives. Discharge patterns are obtained on the surface of an insulator. Organic fibers are etched. Thermosetting polyimide is consolidated. The structure of insoluble polymonomethylsilane is rearranged into that of the soluble polymonomethylsilane. A single crystal of $CoSb_3$ is grown from the compound powder by slow heating. Eutectics solidified from the eutectic powders keeps their original structures.

2. Innovative materials

2.1. Sintering Al metal and alloy

Al particles are covered with aluminum oxide film, and cannot be sintered by normal and hot press sintering. The oxide film cannot be broken and/or removed by heat. The powders can be forged into a dense body under heating conditions.

The properties of the Al alloy (Si 25 wt.%, Fe 3.5 wt.%, Ni 3.5 wt.%, Mg 1 wt.%) sintered by SPS are shown together with that of the forged alloy in Table 1 [7]. The properties of these two are almost same. The oxide film of the Al alloy cannot be removed completely, and persists in the sintered product. The plasma of SPS only makes holes in the film. It is not clarified how the plasma is generated in the graphite die. It is said that the plasma occurs near contact points of powders. The plasma point cannot settle down in any one place, but wanders about. The interval of the plasma generation corresponds to the pulse of the current. The energy of spark plasma is weak at each point. For the generation of the plasma, the powders must be pressed, because the high resistance of loose contact of die alignment does not allow the passage of electric current. The combined force of weak plasma and stress enables the creation of small holes in the oxide film. The diffusion of Al commences through these holes.

Table 1
Properties of Al alloy compacts formed by SPS (12 current pulses and two off-current pulses) and forging

Method	Bulk density (kg/m^3)	Hardness HrB/Hv (1N)
SPS	2740	93.2/188
Forging	2790	88-92/160-180

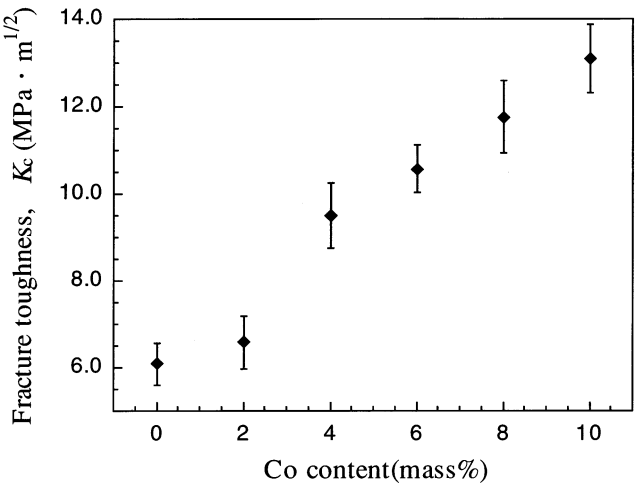

Fig. 1. Fracture toughness of WC and WC–Co bodies.

2.2. Sintering pure WC powder

Production of WC masses is difficult without sintering additives. Dense compacts have been synthesized by the addition of Co, Fe and Ni [8]. WC–Co cemented carbide is valuable for use in cutting tools and dies, because its strength [9] and toughness [10,11] increase with increasing Co content. The hardness of the WC–Co system is lowered compared with that of the pure WC by the addition of Co [11]. A hard WC body is required for some kinds of tools. However, it is difficult to sinter WC using hot pressing.

Pure WC powders are consolidated by SPS above 1900°C [12]. Vickers hardness is 24 GPa. Fig. 1 shows the relationship between fracture toughness and the amount of Co when using SPS. The toughness of 6 $MPa{\cdot}m^{1/2}$ is considerably high [13], and the bending strength is 950 MPa. The pure WC body is an excellent ceramic with applications to tools and machine parts. WC powders contain Cr of 0.8 wt.% to inhibit grain growth. When the powder free from Cr is heated for a few minutes at 1900°C and for 20 min from 20 to 1900°C, the grain is enlarged by 1 mm. The SPS process does not result in fine structures on this heating schedule. It is said that the rapid sintering by SPS depresses the grain growth of polycrystals. When the consolidation is completed by a few minutes, including heating and keeping processes, the grains could be small. The rapid consolidation is confronted by the formation of inhomogeneous compacts. The usual process takes 20–40 min from start to finish, and affords a grain structure of ordinary size. There is no clear reason why WC powder can not be sintered by hot pressing. The crystal structure of WC is a layer-by-layer structure of W and C. C layers that appear on the surface of particles might be not joined or might disturb the diffusion of materials. A part of carbon is spattered by spark plasma, and W layers are revealed.

2.3. Sintering pure AlN powder

AlN powders are sintered without additives above 1800°C. Full densification is achieved with more than 2 wt.% oxygen by hot pressing. The self-diffusion coefficient (D) of AlN increases with increasing oxygen

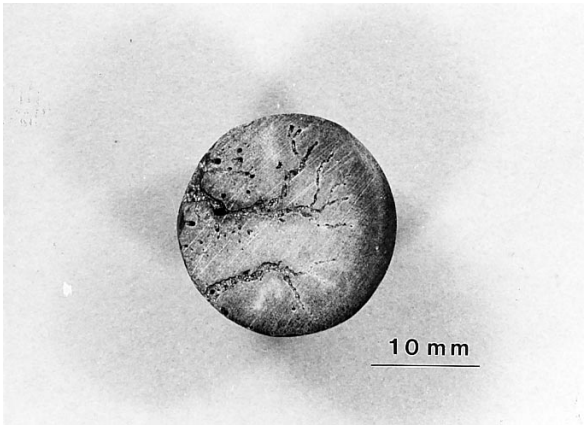

Fig. 2. Electric discharge pattern on the surface of $CeSiNO_2$.

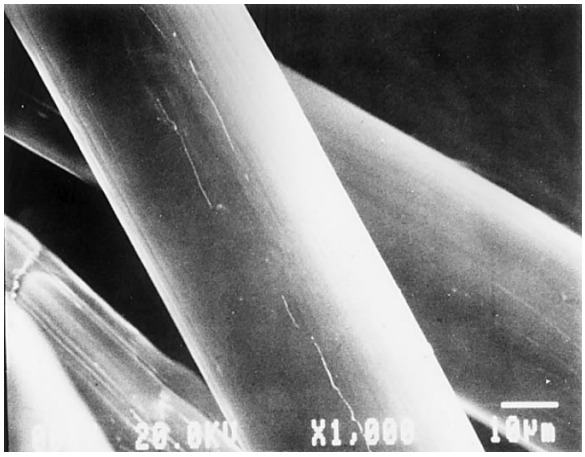

Fig. 3. SEM image of polyethylene fiber.

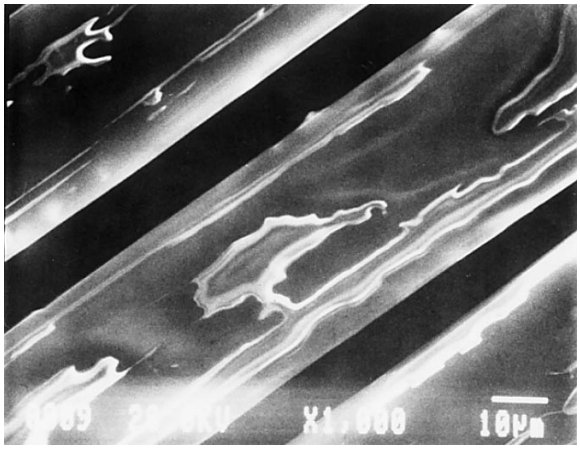

Fig. 4. SEM image of the polyethylene fiber exposed to electrical discharge in air.

content. Cation vacancies are introduced in AlN crystals by oxygen doping, and assist the solidification of AlN powders [14]. The sintering process of AlN is primarily based on vacancy diffusion.

AlN powder with less than 1 wt.% oxygen is sintered into near-theoretical density in a short period by SPS [15–17]. Oxides are not observed at grain boundaries and seem to be removed partially. There are two possible explanations for the formation of the dense AlN. Numbers of vacancies are few for low-oxygen powders. The diffusion of vacancies is accelerated by the electric field of direct current of SPS. The rapid diffusion is as valuable as the presence of many more vacancies. Another reason is that the plasma enhances the reaction of oxygen and AlN, and introduces vacancies. If vacancy diffusion is rate determining for the consolidation, it is likely that the sintering rate of pure AlN powders is accelerated by electric field and/or spark plasma.

2.4. Discharge pattern on an insulator surface

The effect of the plasma is remarkable at the initial stage of sintering, because there are many gaps in the powder. The plasma sites are gradually reduced with decreasing porosity on the middle stage of sintering, and are not generated when the gaps disappear. The melting point of an insulator ($CeSiNO_2$) is near the sintering temperature. The heat treatment with SPS is controlled observing the shrinkage of the samples. In the case of $CeSiNO_2$, it is hard to judge when sintering has been completed. Samples shrink until the densification is achieved. After the shrinkage stops at a certain temperature, the sample starts to melt simultaneously in the small area between the sample and the graphite punch. Gaps appear in the melt, and the spark plasma is regenerated there. As the site of plasma generation is limited, the plasma is concentrated only on the melted area. The plasma increases the melt, and leaves some patterns on the surface, as shown in Fig. 2 [18].

2.5. Etching organic fibers

Discharge chemistry consists of reactions, etching and abrasion. These are caused by non-disruptive or low-energy discharges. Disruptive discharges deteriorate organic compounds, and produce acetylene finally. Ionized ions and radicals are created in the plasma. Radical-initiate reactions and charge-exchange and ion-molecule reactions occur for organic compounds in plasma [19,20].

Surfaces of organic fibers, polyethylene and polypropylene are etched by spark plasma [18]. These fibers are exposed to a discharge in the graphite die for 3 s. The atmosphere of the discharge can be selected from air, N_2, Ar, and vacuum, and is responsible for the etching. The discharged fibers lose their luster. SEM images of the raw and discharged fibers are shown in Figs. 3–6. Polyethylene fibers are worn off from superficial layers in a short period. The plasma does not penetrate into the fiber. The point of plasma generation of polyethylene runs on the surface, or the surface is

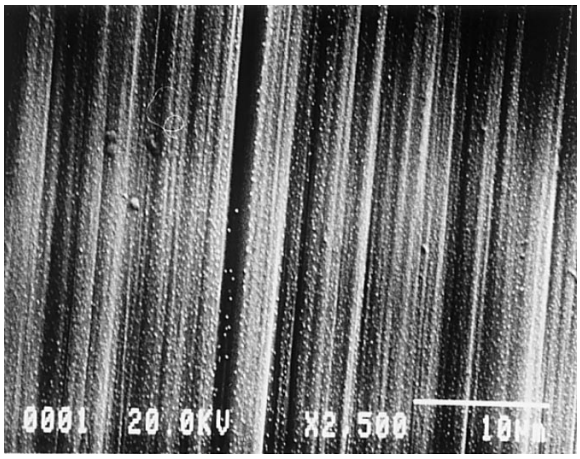

Fig. 5. SEM image of polypropylene fiber.

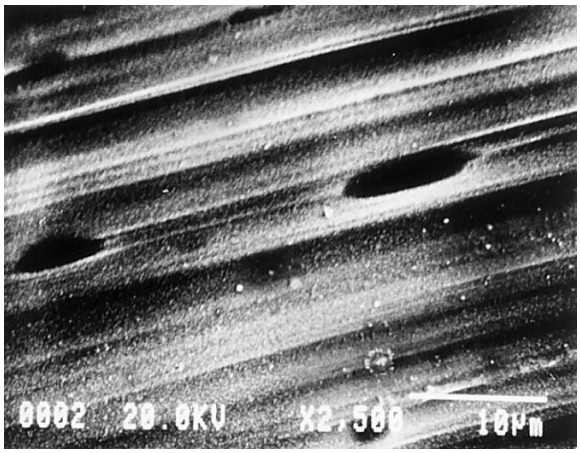

Fig. 6. SEM image of the polypropylene fiber exposed to electrical discharge in N_2.

fragile with respect to the abrasion of radicals and ionized ions. The etched area of polypropylene is localized. The remaining surface, except for the etched hole, keeps its original appearance. Spark plasma is generated at certain points near the place of contact. The spark plasma process does not make new bonds connecting fibers.

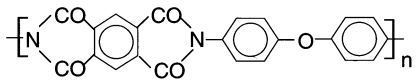

Fig. 7. Chemical structure of polyimide.

2.6. Consolidation of thermosetting polyimide

Thermoplastic polyimide, which has excellent formability, has been used as insulation film for electrical and electronic applications, because of its thermal stability and toughness [21]. Densely consolidated thermosetting polyimide has not been obtained by heating and hot pressing. The application of the thermosetting is restricted.

Thermosetting polyimides have been consolidated by SPS [22]. The consolidation temperature of the thermosetting polyimide depends on the applied pressure, as shown in Table 2. The polyimide, which is consolidated at 380°C and at 19.6, 29.4 and 39.2 MPa, is partially carbonized, becoming dark and brittle. Polyimides are heat-resistant over 400°C, and cannot be carbonized at this temperature. The energy of plasma may be larger at high pressure than at low. Polyimide is partially deteriorated under high pressure at 380°C. The temperature is lowered gradually from 380 to 200°C at 9.8, 19.6, 29.4, 39.2, and 147 MPa to avoid carbonization. The consolidation of the normal color is achieved at the temperatures listed in Table 2. Densities, elastic moduli and thermal expansion coefficients of the consolidated polyimide are shown in Table 2. The Young's modulus obtained is similar to that of the bulk of polymethyl methacrylate [23]. Thus, the densification is sufficient for structural use. The spark plasma excites certain bonds such as imide and ether groups which are shown in Fig. 7, and then new chemical bonds are formed, resulting in cemented structures. These effects on polymers suggest that the spark plasma energy should be weak so as not to damage the polymer structures, but sufficient to excite chemical bonding.

Table 2
Consolidation of polyimide by SPS

Pressure (MPa)	9.8	19.6	29.4	39.2	147
Consolidation temp. (°C)	380	290	290	215	200
Bulk density (g cm^{-3})	1.06	1.27	1.33	1.34	1.44
Poisson's ratio	0.305	0.345	0.360	0.359	0.397
Young's modulus (GPa)	1.45	3.00	3.15	3.17	4.40
Shear modulus (GPa)	0.556	1.12	1.16	1.17	1.57
Bulk modulus (GPa)	1.24	3.22	3.72	3.74	7.15
Thermal expansion coefficient (10^{-6} K^{-1})	50.7	47.6	50.6	51.8	49.3

2.7. Structure rearrangement of polymonomethylsilane

Dimethyldichlorolsilane composed of two carbon atoms and a silicon atom is polymerized to polysilane using Na. Polysilane, which is not soluble in organic solvents and does not melt, is rearranged to polycarbosilane by heating at over 400°C. Raw fibers are spun from polycarbosilane. SiC fibers are fabricated by heat treatment of the raw fibers at about 1300°C [24]. The SiC fiber is a composite consisting of SiC and C.

Monomethyltrichlorosilane is an ideal material for the formation of SiC, because it contains equal amounts of Si and C. Polymonomethylsilane polymerized from monomethylsilane does not melt, and is not soluble in organic solvents. It is impossible to rearrange this polysilane into the soluble form by heating. However, the rearrangement can be achieved in a vacuum by SPS and produces a soluble polymer [25].

Polymonomethylsilane is a cross-linked polymer, as shown in Fig. 8. Methyl groups are bonded as side chains. After the bond of Si–Si is broken, a new bond of Si–C is created in main chains. Silane and methylene radicals are formed from Si–Si bonds and methyl groups by spark plasma. These radicals make new Si–C bonds. The rearranged polymer consisting of the Si–C bond melts and become soluble in organic solvents.

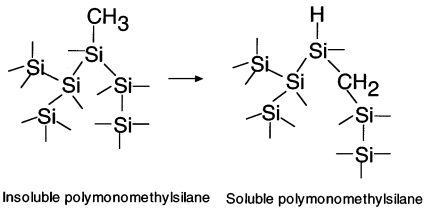

Fig. 8. Structure rearrangement of polymonomethylsilane.

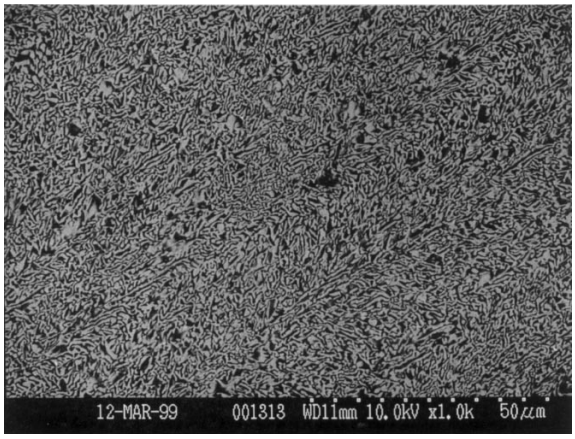

Fig. 9. SEM image of the eutectic (Al_2O_3–$Y_3Al_5O_{12}$) melted by arc discharge.

2.8. Crystal growth of $CoSb_3$

A thermoelectric device of Bi_2Te_3 can be applied to the cooling devices of refrigerators to replace compressors. The maximum dimensionless figure of merit ZT of Bi_2Te_3 is near room temperature. Compounds of a skutterudite group ($CoAs_3$, $RhAs_3$, $CoSb_3$, $RhSb_3$ and $IrSb_3$) possess good potential for achieving ZT values substantially larger than those of state-of-the-art thermoelectric materials at high temperatures. Very heavily doped n-type $CoSb_3$ can achieve $ZT \approx 1$ at 600°C [26]. The compound of $CoSb_3$ is peritectic. A single crystal can be grown from a Sb-rich melt [27]. The growth takes considerable time and needs advanced techniques.

The mixture of Co and 3Sb is reacted at 550°C for 48 h. The ground powders are put in a graphite die with a diameter of 20 mm, and then heated at 1°C/min from 600 to 720°C in Ar gas. A single crystal with a diameter of 8 mm can be obtained [28]. The growth direction is not aligned along the electric field. Skin current on crystals of semiconductors may promote crystal growth.

2.9. Crystal growth of eutectics

Structures of eutectic composites are quite different from those of ordinary composites [29–31]. Two single crystals are grown unidirectionally to be intertwined each other. The crystal growth has been achieved by a modified Bridgman technique using crucibles [30,32,33]. Floating zone melting can achieve the coupled unidirectional growth without crucibles [34,35]. Attention to eutectics has been concentrated on potential electrical, magnetic, and mechanical applications. Advanced gas turbine blades are expected to be prepared from eutectic composites, because of the high melting points, high strength-to-weight ratios at high temperatures, and resistance to oxidation [30]. A eutectic with large crystals of 30 μm in width keeps its strength until 1973 K [36]. In the case of Bridgman crystal growth, coupled unidirectional solidification is carried out using crucibles. The product size is regulated by the capacity of the crucibles. The volume of melt of floating zone growth must be small, because it is sustained by the surface tension of the melt. Large diameter crystals cannot be fabricated from a small amount of melt. There are another disadvantages for crystal growth: the growth rate is slow, it is impossible to form near-net-shape products, and the eutectic prepared by unidirectional solidification possesses considerable crystallographic anisotropy. These problems must be solved by the application of powder metallurgy methods. However, eutectic powder has not been solidified by normal sintering and hot pressing.

Calcined powders of the eutectic composition of Al_2O_3–$Y_3Al_5O_{12}$ (YAG) are melted by arc discharge.

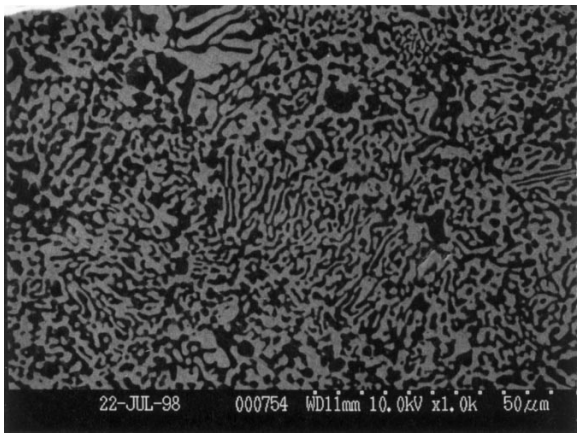

Fig. 10. SEM image of the eutectic (Al_2O_3–$Y_3Al_5O_{12}$) consolidated by SPS.

The melt is cooled and rapidly solidified. The cooling rate is not uniform throughout melt. The crystal size of the eutectic varies from fine and coarse. Fig. 9 shows that mainly fine structures are produced in an orderly fashion. The finest eutectic structure is less than 0.3 μm in width. The white phase YAG, and the black is Al_2O_3. The largest crystals are less than approximately 10 μm in size.

The eutectic powder is consolidated by SPS. The structure of the solidified eutectic is shown in Fig. 10. Pores and the structure of composites are not observed. It seems that small units of the eutectic are joined and that crystal alignment is not present. Each coupled crystal of YAG and Al_2O_3 is grown respectively by SPS. The color of YAG bodies sintered by SPS is gray or black, indicating the formation of oxygen vacancies. On the other hand, the alumina bodies are white and do not lose much of oxygen. There is a recognized difference of oxygen vacancies between YAG and Al_2O_3 bodies. Oxygen vacancies may serve to connect individual crystals in the electric field [37]. The electric field may identify the difference and connect the crystals.

References

[1] M. Tokita, J. Soc. Powder Tech. Jpn. 30 (1993) 790–804.
[2] M. Ishiyama, Plasma activated sintering (PAS) system, in: Y. Bando, K. Kosuge (Ed.), Proceedings of the 1993 Powder Metall. World Congress, Kyoto, Jpn. Soc. Powder & Powder Metall. Japan, 1993, pp. 931–934.
[3] K. Inoue, US Patent, No. 3 241 956 (1966).
[4] K. Inoue, US Patent, No. 3 250 892 (1966).
[5] R.W. Boesel, M.I. Jacobson, I.S. Yoshioka, Mater. Eng. 70 (1969) 32–35.
[6] Y. Furuya, R. Watanabe, H. Yaguchi, M. Saito, T. Kubo, T. Abe, M. Omori, Preparation of smart composites by SPS, Proceedings of the Third Symposium on Spark Plasma Sintering, Kure, Japan, 1998, pp. 42–45.
[7] T. Nagae, M. Nose, M. Yokota, J. Jpn. Soc. Powder & Powder Metall. 43 (1993) 1193–1197.
[8] K. Schreoter, US Patent, No. 1 549 615 (1925).
[9] J. Gurland, P. Bardzil, J. Met. 7 (1955) 311–315.
[10] H.E. Exner, Trans. Metall. Soc. AIEM 245 (1969) 677–683.
[11] P. Kenny, Powder Metall. 14 (1971) 22–39.
[12] S. Suzuki, Fabrication of hard metal, Proceedings of the First Symposium on Spark Plasma Sintering, Sendai, Japan, 1996, pp. 13.
[13] M. Omori, T. Kakita, A. Okubo, et al., J. Jpn Inst. Met. 62 (1998) 986–991.
[14] T. Sakai, M. Iwata, J. Mater. Sci. 12 (1977) 1659–1665.
[15] J.R. Groza, S.H. Risbud, K. Yamazaki, J. Mater. Res. 7 (1992) 2643–2645.
[16] J.E. Hensley, S.H. Risbud, J.R. Groza, et al., J. Mater. Eng. Perform. 2 (1993) 665–669.
[17] S.H. Risbud, J.R. Groza, M.J. Kim, Phil. Mag. B 69 (1994) 525–533.
[18] M. Omori, T. Hirai, Material and composite formation by spark plasma system (SPS), in: M. Miyake, M. Samandi, Proceedings of the First Symposium on Microwave, Plasma and Thermochemical Processing of Advanced Materials, Osaka University, Japan, 1997, pp. 50–56.
[19] F.K. McTaggart, Plasma Chemistry in Electrical Discharges, Elsevier, Amsterdam, 1967.
[20] J.R. Hollahan, A.T. Bell (Eds.),Chemical Reactions in Electrical Discharges, Wiley, New York, 1974.
[21] C.E. Sroog, J. Polym. Sci. Macromol. Rev. 11 (1976) 161–208.
[22] M. Omori, A. Okubo, K. Gilhwan, et al., J. Mater. Synth. Proc. 5 (1997) 279–282.
[23] M. Fukuhara, A. Sampei, J. Polym. Sci. Polym. Phys. 33 (1995) 1847–1850.
[24] S. Yajima, J. Hayashi, M. Omori, Chem. Lett. 9 (1975) 931–934.
[25] M. Matsuda, A. Watanabe, T. Hirai and M. Omori, Japanese patent, Tokugan-hei 5-77365 (1993).
[26] J.–P. Fleurial, T. Caillat, A. Borshchevsky, Skutterudites: an update, A. Heinich, J. Schumann (Eds.) Proceedings of the 16th International Conference on Thermoelectrics, The Institute of Electrical and Electronics Engineers, USA, 1997, pp. 1–11.
[27] T. Caillat, J.-P. Fleurial, A. Borshchevsky, J. Cryst. Growth 166 (1996) 722–726.
[28] T. Koyanagi, Preparation of thermoelectric material by spark plasma sintering, Proceedings of the Third Symposium on Spark Plasma Sintering, Kure, Japan, 1998, pp. 54–55.
[29] F.S. Galasso, J. Met. 19 (1967) 17–21.
[30] C.O. Hulse, J.A. Batt, Effect of Eutectic Microstructures on the Mechanical Properties of Ceramic Oxides, Final Tech. Rept. UARL-N910803-10, May 1974; NTIS AD-781995/6GA; 140 pp.
[31] V.S. Stubican, R.C. Bradt, Ann. Rev. Mater. Sci. 11 (1981) 267–297.
[32] D.E. Harison, J. Cryst. Growth 3 (1968) 674–678.
[33] D. Viechnicki, F. Schmid, J. Mater. Sci. 4 (1969) 84–88.
[34] F.S. Galasso, W.L. Darby, F.C. Douglas, et al., J. Am. Ceram. Soc. 50 (1967) 333–334.
[35] G. Dhalenne, A. Revcolevschi, R. Collongues, Mater. Res. Bull. 7 (1972) 1385–1392.
[36] Y. Waku, H. Ohtsubo, N. Nakagawa, et al., J. Mater. Sci. 31 (1996) 4663–4670.
[37] M. Omori, T. Isobe, T. Hirai, Consolidation of Eutectic powder by SPS, unpublished data.